Journal of Computational Applied Mechanics 2022, 53(4): 510-523

DOI 10.22059/jcamech.2022.348183.753

RESEARCH PAPER

Effect of Electric Field Modulation on the Onset of Electroconvection in an Anisotropic Porous Layer Saturated with a Dielectric Fluid

Rudresha C, Balaji C, Vidya Shree V, Maruthamanikandan S

Department of Mathematics, School of Engineering, Presidency University, Bengaluru 560064, India

Abstract

The method of small perturbation coupled with the regular perturbation method is employed to investigate the effect of time-periodic electric field modulation on electroconvection in a densely packed anisotropic porous layer saturated with a Boussinesq dielectric fluid. The Darcy model is adopted to describe the fluid motion and the dielectric constant is assumed to be a linear function of temperature. The regular perturbation method is used to determine the critical correction Rayleigh number for small amplitude electric field modulation. It is shown that electric field modulation frequency, electrical, porosity, and anisotropic parameters are related to the shift in the critical Rayleigh number and that subcritical convective motion is possible for low frequency modulation of the electric field. The classical destabilizing effect of the dielectrophoretic force associated with the unmodulated, anisotropic dielectric fluid porous layer is only realized for low frequency modulation of the electric field. Furthermore, it is substantiated that anisotropic parameters greatly influence the stability criterion for moderate and large values of the frequency of electric field modulation. The study reveals that time-varying electric fields and anisotropic characteristics of the fluid layer may have implications for the control of electroconvection in heat transfer applications involving dielectric fluid as working media.

Keywords: Anisotropic Porous Medium, Dielectric Fluid, Electric Field, Modulation, Porosity.

1. Introduction

As for dielectric fluids, temperature gradients cause dielectric constant and electrical conductivity to vary. Free charge is accumulated in the fluid when a *dc* electric field is applied. The rate of accumulation increases exponentially during the accumulation of constant free charges. This constant is called the electrical relaxation time. The free charge has no time to build up when an electric field of alternating current is applied at a frequency that is substantially higher than the reciprocal of the electrical relaxation time. At typical power line frequencies, free charge effects appear to be insignificant for the majority of dielectric fluids due to their lengthy electrical relaxation durations. Dielectric loss is also so negligible at these frequencies that it has no impact on the temperature field. Furthermore, because body force changes so quickly, the mean value can be taken as the effective value for calculating fluid motions, with the exception of fluids having extremely low viscosities [1-4].

Castellanos *et al.* [5] examined the impact of altering the dielectric constant and ionic mobility at various temperatures on the stability of a horizontal dielectric liquid layer subjected to an electric field and heating from below. The stability of natural convection of an electrically conducting fluid between two parallel vertical plates kept at constant and different temperatures and permeated by a transverse magnetic field was investigated by

Takashima [6] using the linear stability theory. Chang and Watson [7] explored the impact of electroconvection on heat transfer, and numerous scholars [8-10] have looked at some related experimental and theoretical studies. Zhiming *et al*. [11] performed a numerical analysis of the dielectric fluid flow in an EHD under the influence of gravitational and Coulomb forces. Periodic forcing on liquids can take the form of vibrations, variations in surface temperature or heat flux, or alternating electric fields. With a wide range of scientific applications, time-dependent forces acting on a fluid can significantly alter instability thresholds and offer a reliable method of controlling convection [12-53].

A few geophysical and technological issues where thermally driven convection in porous media is significant include the modelling of geothermal reservoirs and thermal insulation systems, packed-bed catalytic reactors, and heat storage devices. Researchers have explored porous media flows' theory and modelling for quite a long time and isotropic porous media has been the primary subject of theoretical and experimental investigations. However, in many practical situations, the mechanical and thermal properties of the porous matrix are anisotropic. A good example of such a medium is loft insulation, which typically has a lower permeability across the insulating layer than it does in the perpendicular direction. According to Wooding [54], in geothermal systems, horizontal permeability might be up to ten times greater than vertical permeability in some circumstances.

Since the 1970s, researchers have focused primarily on the porous medium equivalent of the Bénard problem, also known as the Lapwood problem, in their studies of natural convection in anisotropic porous media. Castinel and Combamous [55] made the discovery of the criterion for the commencement of convection in an anisotropic layer. Additionally, they revealed experimental findings that mostly corroborated their theoretical forecasts. By including anisotropy in the thermal diffusivity, Alex and Patil [56] extended the stability investigation. It has been established that the marginal stability criterion and the required width of the convection cells are both influenced by anisotropy in the mechanical and thermal properties. Malashetty and Basavaraja [57] provided evidence for the interaction between the anisotropy of the porous medium, time-dependent wall temperature, and gravity modulation on the onset of convection. The stability of the system has been discovered to be significantly affected by even minor anisotropic properties. Malashetty and Biradar [58] studied the double-diffusive convection in a horizontal couple stress fluid saturating an anisotropic porous layer. It is discovered that stationary, oscillatory, and finite amplitude convection are all delayed by the thermal anisotropy parameters. Rayleigh-Bénard convection in a porous medium with ferromagnetic fluid and a time-varying gravity field has been studied by Thomas and Maruthamanikandan [59]. They concentrated on how a porous matrix and gravity modulation might alter the stability necessary for the initiation of ferroconvection. Shamsudin and Mokhtar [60] investigated the impact of anisotropy on the electrothermal instability in a porous medium with nanofluid in the presence of a vertical *ac* electric field.

Takashima and Hamabata [61] investigated spontaneous convection in a vertical layer of dielectric fluid in the presence of a horizontal *ac* electric field. It is shown that electric force has no impact on the natural convection stability mechanism when the electrical Rayleigh number is less about 2130. In a transverse electric field, Semenov [62] studied the parametric instability of a horizontal layer of liquid dielectric that has not been uniformly heated and has free isothermal boundaries. It is shown that instability can happen in a critical electric field strength that is several orders of magnitude higher than the critical strength of a constant electric field. The electrothermoconvective instability of a plane horizontal layer of poorly conducting fluid in a modulated vertical electric field is the subject of research by Velarde and Smorodin [63]. It has been demonstrated that modulation can either sustain or destabilize fluid equilibrium depending on the amplitude and frequency. Rudresha *et al*. [64] investigated the impact of electric field modulation on electroconvection in a porous material. They showed that effects of electric field modulation and porous medium are mutually antagonistic at low frequencies of electric field modulation.

Thermo-electroconvection in a dielectric fluid subjected to time-periodic electric field modulation with couple stresses has been investigated by Rudresha *et al*. [65]. It is shown that the stability of the system is strongly influenced by the couple stress parameter and the Prandtl number diminishes the stabilizing impact of couple stresses. The current study addresses how electric field modulation and anisotropic properties affect the stability criterion associated with the onset of electroconvection. The perturbation approach is used to determine the critical Rayleigh number and the associated wavenumber provided the amplitude of electric field modulation is of modest magnitude. The amplitude and frequency of the modulation are externally controlled parameters and hence the onset of electroconvection can be delayed or advanced by the proper tuning of these parameters. The problem has potential applications in achieving major enhancement of mass, momentum and heat transfer in the geothermal context and related areas.

2. Mathematical formulation

The electric force which acts on the dielectric fluid per unit volume is expressed in the form [6]

$$\vec{f}_e = \rho_e \vec{E} + \nabla \cdot \left(\frac{1}{2} \rho \frac{\partial \varepsilon_d}{\partial \rho} \left(\vec{E} \cdot \vec{E} \right) \right) + \frac{1}{2} \left(\vec{E} \cdot \vec{E} \right) \nabla \varepsilon_d \,. \tag{1}$$

In the above equation, $\vec{E}$ is the electric field, ρ_e is the free electric charge density, ε_d is the dielectric constant and ρ is the fluid mass density. The first term $\rho_e \vec{E}$ indicates the Coulomb force, while the second and third terms indicate the non-uniformities in the dielectric constant. Under a 60-Hz *ac* electric field, the Coulomb force is of insignificant order when compared with the dielectrophoretic force in the vast majority of dielectric fluids. As a result, we ignore the Coulomb force term and just keep the dielectrophoretic term. Additionally, dielectric liquids appear to have long electrical relaxation durations at common power line frequencies, which prevent free charges from developing. As a result, the dielectric loss has a little effect on the temperature field at these frequencies.

The densely packed porous layer of dielectric fluid is confined to an infinitely long horizontal porous layer with surfaces at $z = 0$ and $z = d$. These boundaries are sustained at constant temperatures $T = T_0$ and $T = T_1$ respectively and modulation electric potential $\phi = \pm U \left(\eta_1 + \eta_2 \cos \omega t \right)$ is retained on the boundaries, where U is the magnitude of the modulation of the electric potential, ω is the frequency of modulation and, η_1 and η_2 are the relative amplitudes of the components of constant and alternating potential difference. An anisotropic porous medium has three co-ordinate axes (*x*, *y*, and *z*) parallel to the main axes of the medium, and the *z*-axis points vertically upward, which is the opposite direction of gravity. Usually, homogeneous anisotropic porous media are homogeneous in two directions parallel to the bedding plane. So, it can be assumed that the bedding plane is isotropic, leading to the horizontal case. Based on the assumption that the permeabilities and thermal diffusivities are equal in the *x* and *y* directions, the *xy* plane has been considered the bedding plane. The relevant governing equations, taking into account that there are neither induced nor applied magnetics forces and invoking the Boussinesq approximation, read [10, 56]

$$\nabla \cdot \vec{q} = 0 \tag{2}$$

$$\frac{\rho_0}{\varepsilon_p} \left[\frac{\partial \vec{q}}{\partial t} + \frac{1}{\varepsilon_p} \left(\vec{q} \cdot \nabla \right) \vec{q} \right] = -\nabla p + \rho \vec{g} - \mu_f \vec{K} \vec{q} - \frac{1}{2} \left(\vec{E} \cdot \vec{E} \right) \nabla \varepsilon_d \tag{3}$$

$$\gamma \frac{\partial T}{\partial t} + \left(\vec{q} \cdot \nabla \right) T = \nabla \left(\kappa_T \nabla T \right) \,. \tag{4}$$

$$\nabla \cdot \left[\varepsilon_d \vec{E} \right] = 0 \tag{5}$$

$$\nabla \times \vec{E} = 0 \Rightarrow \vec{E} = -\nabla \phi \tag{6}$$

$$\rho = \rho_0 \left[1 - \alpha \left(T - T_0 \right) \right] \tag{7}$$

$$\varepsilon_d = \varepsilon_0 \left[1 - e \left(T - T_0 \right) \right] \tag{8}$$

where $\vec{q} = (x, y, z)$ is the velocity vector, T is the temperature, ε_d is the dielectric constant, e is the expansion coefficient of dielectric constant (always positive), α is the thermal expansion coefficient, $\vec{E}$ is the electric field, $\vec{g}$ is the gravitational acceleration, ϕ is the electric potential, p is the pressure, ρ is the density of the fluid, μ_f is the fluid viscosity, ρ_0 is the density at reference temperature, ε_0 is the electrical permittivity, ε_p is the porosity of the porous medium, $\vec{K} = K_x^{-1}\left(\hat{i}\hat{i} + \hat{j}\hat{j}\right) + K_z^{-1}\left(\hat{k}\,\hat{k}\right)$ is the anisotropic permeability tensor with K_x and K_z being the permeabilities of the porous medium in the horizontal and vertical directions respectively, $\kappa_T = \kappa_{Tx}\left(\hat{i}\hat{i} + \hat{j}\hat{j}\right) + \kappa_{Tz}\left(\hat{k}\,\hat{k}\right)$ is the anisotropic thermal diffusivity tensor with κ_{Tx} and κ_{Tz} being the thermal diffusivities in the horizontal and vertical directions respectively, and $\gamma = \dfrac{(\rho c)_m}{(\rho c)_f}$ is the ratio of specific heats.

3. Basic state

The basic state of the system is taken to be a quiescent layer and is given by

$$\left.\begin{aligned} &\frac{\partial}{\partial t} = 0; \quad \vec{q} = \vec{q}_b(z) = 0; \quad T = T_b(z); \quad p = p_b(z); \quad \rho = \rho_b(z); \\ &\qquad \varepsilon_d = \varepsilon_{d_b}(z); \quad \phi = \phi_b(z); \quad \vec{E} = \vec{E}_b = \left[0, 0, E_b(z)\right] \end{aligned}\right\} \tag{9}$$

where suffix *b* represents the basic state. Using equation (9) in equations (2) through (8), we obtain

$$\vec{0} = -\nabla p_b + \rho_b\,\vec{g} - \frac{1}{2}E_b^2\,\nabla\varepsilon_{d_b} \tag{10}$$

$$T_b = T_0 - \beta z \tag{11}$$

$$\rho_b = \rho_0\left[1 + \alpha\beta z\right] \tag{12}$$

$$\varepsilon_{d_b} = \varepsilon_0\left[1 + e\beta z\right] \tag{13}$$

$$\phi_b = -E_0 \log\left(1 + e\beta z\right) + U\left(\eta_1 + \eta_2 \cos\omega t\right) \tag{14}$$

and

$$E_b = \frac{2U\left(\eta_1 + \eta_2\cos\omega t\right)}{d}\left(1 - e\beta z\right) \tag{15}$$

with $E_0 = \dfrac{2U\left(\eta_1 + \eta_2\cos\omega t\right)e\beta}{\log\left(1 + e\beta d\right)}$ and $\beta = \dfrac{T_0 - T_1}{d}$.

4. Linear Stability Analysis

We study the stability of this basic state using the method of small perturbations. On the basic state we superpose infinitesimal perturbations of the form

$$\left.\begin{aligned} &\vec{q} = \vec{q}\,' = \left(u', v', w'\right); \quad p = p_b + p'; \quad T = T_b + T'; \\ &\varepsilon_d = \varepsilon_{d_b} + \varepsilon'; \quad \phi = \phi_b + \phi'; \quad \vec{E} = \vec{E}_b + \vec{E}'. \end{aligned}\right\} \tag{16}$$

Using (16) in equations (2) through (8) and following the standard stability analysis [4, 56, 64], we obtain

$$\frac{\rho_0}{\varepsilon_p}\frac{\partial}{\partial t}\left(\nabla^2 w'\right)=\alpha\rho_0 g\nabla_1^2 T'-\frac{\mu_f}{K_z}\left(\nabla_1^2 w'+\frac{K_z}{K_x}\left(\frac{\partial^2 w'}{\partial z^2}\right)\right)+\frac{L_1 e\beta\varepsilon_0}{d}\frac{\partial}{\partial z}\left(\nabla^2\phi'\right)+\frac{L_1^2 e^2\beta\varepsilon_0}{d^2}\nabla_1^2 T' \tag{17}$$

$$\nabla^2\phi'=\frac{-2U\left(\eta_1+\eta_2 f\right)e}{d}\frac{\partial T'}{\partial z} \tag{18}$$

$$\gamma\frac{\partial T'}{\partial t}-\beta w'=\kappa_{Tx}\nabla_1^2 T'+\kappa_{Tz}\frac{\partial^2 T'}{\partial z^2} \tag{19}$$

where $L_1=2U\left(\eta_1+\eta_2\cos\omega t\right)$, $\nabla_1^2=\left(\partial^2/\partial x^2+\partial^2/\partial y^2\right)$, $\nabla^2=\left(\partial^2/\partial x^2+\partial^2/\partial y^2+\partial^2/\partial z^2\right)$ and $f=\cos\omega t$. Equations (17) through (19) are made dimensionless by means of the following transformations $T^*=T'/\beta d$, $t^*=\kappa_{Tx}/d^2$, $\left(x^*,y^*,z^*\right)=\left(x/d,\ y/d,\ z/d\right)$, $w^*=w'd/\kappa_{Tz}$ and $\phi^*=\phi'/eL_1\Delta T$. As a result, we obtain the following dimensionless equations (after dropping the asterisks for simplicity)

$$\left(\frac{1}{P_{rD}}\frac{\partial}{\partial t}\nabla^2+\left(\nabla_1^2+\frac{1}{\varepsilon}\frac{\partial^2}{\partial z^2}\right)\right)w=\left[R_T+R_{et}\left(1+\eta_3 f\right)^2\right]\nabla_1^2 T+R_{et}\left(1+\eta_3 f\right)^2\frac{\partial}{\partial z}\nabla_1^2\phi \tag{20}$$

$$\nabla^2\phi=-\frac{\partial T}{\partial z} \tag{21}$$

$$\left(\frac{\partial}{\partial t}-\left(\eta\nabla_1^2+\frac{\partial^2}{\partial z^2}\right)\right)T=w \tag{22}$$

where $R_T=\dfrac{\alpha\rho_0 g\beta K_z d^2}{\mu_f\kappa_{Tz}}$ is the Darcy-Rayleigh number, $P_{rD}=\dfrac{\varepsilon_p P_r}{\nu Da}$ is the Darcy-Prandtl number, $R_{et}=\dfrac{4e^2U^2\beta^2\varepsilon_0\eta_1^2 K_z}{\mu_f\kappa_{Tz}}$ is the Darcy-Electrical Rayleigh number, $\eta_3=\dfrac{\eta_2}{\eta_1}$ is the ratio of amplitudes associated with the electrical potential difference, $\nu=\dfrac{\mu_f}{\rho_0}$ is the kinematic viscosity of the fluid, $Da=\dfrac{K_z}{d^2}$ is the Darcy number, $\mathrm{P}_r=\dfrac{\nu}{\kappa_{Tz}}$ is the Prandtl number, $\varepsilon=\dfrac{K_x}{K_z}$ is the mechanical anisotropy parameter and $\eta=\dfrac{\kappa_{Tx}}{\kappa_{Tz}}$ is the thermal anisotropy parameter. Combining equations (20) – (22) yields

$$\left[\left(L_2+L_4\right)L_3\right]\nabla^2 w=\left[R_T\nabla^2+R_{et}\nabla_1^2(1+\eta_3 f)^2\right]\nabla_1^2 w \tag{23}$$

where $L_2=\dfrac{1}{P_{rD}}\dfrac{\partial}{\partial t}\nabla^2$, $L_3=\gamma\dfrac{\partial}{\partial t}-\left(\eta\nabla_1^2+\dfrac{\partial^2}{\partial z^2}\right)$ and $L_4=\nabla_1^2+\dfrac{1}{\varepsilon}\dfrac{\partial^2}{\partial z^2}$.

Keeping in mind the dielectric fluid saturated anisotropic porous layer obeying the Darcy law, we use the impermeable condition for velocity (*i.e.*, normal component of velocity vanishes at the boundaries) and isothermal conditions for temperature. The stress-free boundary conditions are chosen for mathematical simplicity without important physical effects being lost qualitatively. It follows that equation (23) must be solved subject to the following dimensionless homogeneous boundary conditions

$$w=\frac{\partial^2 w}{\partial z^2}=\frac{\partial^4 w}{\partial z^4}=0 \text{ at } z = 0,\ 1 \tag{24}$$

Equation (23) along with boundary conditions (24) is a homogeneous system and thus constitutes an eigenvalue problem.

5. Perturbation Procedure with small Amplitude Approximation

The essential idea of perturbation theory is to find an analytic approximation to solutions of equations. The solution is represented based on the assumption that a small parameter must exist in the equation. Perturbation theory leads to an expression for the desired solution in terms of a formal power series in small parameter known as perturbation series that quantifies the deviation from the exactly solvable problem. The leading order terms describe the deviation in the solution. The eigenvalues and eigenfunctions of the problem at hand are distinct from those of the classical unmodulated electroconvection problem by a quantity of order η_3. As a result, equation (23) has a solution of the form [64]

$$\left.\begin{aligned} w &= w_0+\eta_3 w_1+\eta_3^2 w_2+\ldots\ldots\ldots\ldots\ldots \\ R_T &= R_{T_0}+\eta_3 R_{T_1}+\eta_3^2 R_{T_2}+\ldots\ldots\ldots\ldots\ldots \end{aligned}\right\} \tag{25}$$

The expression for the critical Rayleigh number corresponding to the study of convection in a horizontal dielectric fluid saturated densely packed anisotropic porous layer subjected to a uniform electric field is given by

$$R_{T_0}=\frac{1}{\alpha^2}\left(\eta\alpha^2+\pi^2\right)\left[\alpha^2+\frac{\pi^2}{\varepsilon}\right]-\frac{R_{et}\,\alpha^2}{\left(\alpha^2+\pi^2\right)}\ . \tag{26}$$

Since we are keen on deciding the worth of the non-zero correction R_{T_2} to R_T, following the analysis of [64], the expression for R_{T_2} is given by

$$R_{T_{2c}}=\frac{2R_{et}^2\,\alpha^6}{\left(\alpha^2+\pi^2\right)}\left[\sum_{n=1}^{\infty}\left(\frac{B_1}{B_1^2+B_2^2}\right)\right] \tag{27}$$

where

$$B_1=\frac{\omega^2}{P_{rD}}\left(n^2\pi^2+\alpha^2\right)^2-\eta\,\alpha^2\left(n^2\pi^2+\alpha^2\right)\left[\alpha^2+\frac{n^2\pi^2}{\varepsilon}\right]-\left(n^2\pi^2+\alpha^2\right)\left[\alpha^2+\frac{n^2\pi^2}{\varepsilon}\right]n^2\pi^2+R_{T_0}\,\alpha^2\left(n^2\pi^2+\alpha^2\right)+R_{et}\,\alpha^4$$

$$B_2=\omega\left\{\frac{1}{P_{rD}}\left[\eta\alpha^2+n^2\pi^2\right]\left(n^2\pi^2+\alpha^2\right)^2+\left[\alpha^2+\frac{n^2\pi^2}{\varepsilon}\right]\left(n^2\pi^2+\alpha^2\right)\right\}.$$

6. Results and Discussion

The effect of a time-varying electric field on the onset of electroconvection in a densely packed anisotropic porous layer is investigated in this paper. The correction Darcy-Rayleigh number $R_{T_{2c}}$ is expressed as a function of the Darcy-electrical Rayleigh number R_{et} , Darcy-Prandtl number P_{rD} , thermal and mechanical anisotropy parameters η and ε respectively. The magnitude of the buoyancy force due to thermal gradient is effectively characterized by the thermal Rayleigh number R_T . Physically, the electric Rayleigh number R_{et} represents the balance of energy released by electric force to the energy dissipation by viscous friction and thermal dissipation. The ratio between porosity, thermal Prandtl number and Darcy number is given by the Darcy-Prandtl number P_{rD} . The thermal anisotropy parameter η represents the relative variation of the thermal diffusivity of the fluid layer in the horizontal and vertical directions. The mechanical anisotropy parameter ε, likewise, represents the relative variation of the permeability of the porous medium in the horizontal and vertical directions.

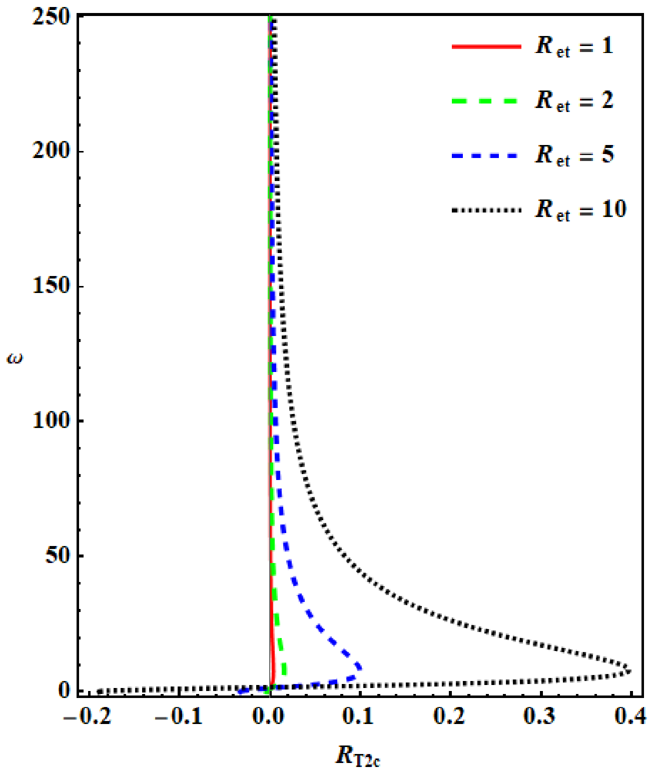

Fig. 1: Plot of $R_{T_{2c}}$ versus ω for different values of R_{et} with $P_{rD} = 2$, $\eta = 0.2$ and $\varepsilon = 0.5$.

It is worth mentioning that the results of this paper are significantly affected by the electric field modulating frequency ω. When ω is small, the period of modulation is long and the electric field modulation affects the fluid boundaries; however, when ω is large, the effect of modulation disappears. This is because the electric force takes a mean value leading to the equilibrium state of the unmodulated case; therefore, we only choose moderate values of ω in the current study. It is observed from Figures 1 through 4 that $R_{T_{2c}}$ is negative for tiny ω. This suggests that electroconvection occurs earlier in the modulated system than in an unmodulated system. However, when ω is moderate or large, $R_{T_{2c}}$ becomes positive, implying delayed convection. When the value of ω is increased further, $R_{T_{2c}}$ decreases and, for large ω, $R_{T_{2c}}$ becomes independent of the frequency of the modulation. This is because when ω is very small, the period of modulation becomes sufficiently large, and the disturbances grow to a large extent, causing the entire system under consideration to become unstable.

Further, we observe from Figures 1 through 4 that in each curve there are two peak values of $R_{T_{2c}}$, one negative and another positive. If ω^* represents the frequency at which $R_{T_{2c}}$ changes its sign from negative to positive, then the modulated system may be classified as destabilized or stabilized, compared with the unmodulated system, according as $\omega < \omega^*$ or $\omega > \omega^*$. First $R_{T_{2c}}$ decreases to its maximum destabilizing value and then increases to its maximum stabilizing value and finally decrease to zero as the frequency increases from zero to infinity. Further, at some particular value of the frequency $\omega = \omega_0$, the effect of modulation disappears entirely, *i.e.*, $R_{T_{2c}} = 0$. Unquestionably, these critical frequencies depend on the values of the other parameters arising in the study.

The analysis presented in this paper is based on the assumption that the modulation amplitude is very small, and the convection currents are weak, allowing nonlinear effects to be ignored. This is equivalent to the fact that the amplitude of $\eta_3 w_1$ should not exceed that of w_0, resulting in the condition $\omega > \eta_3$. As a result, the validity of the results obtained in this paper is dependent on the modulation frequency. The electric field modulation impacts the entire volume of the fluid when ω is sufficiently low (*i.e.*, the period of modulation is large). As a result, the disturbance becomes larger. The effect of modulation is only present in a thin border layer close to the boundary, though, for large values of ω. This is because a renormalization of the static electric field occurs at high frequencies. Due to the electric force taking on a mean value at these thicknesses, the unmodulated scenario reaches its equilibrium state. Therefore, the modulation effect is only notable for small and moderate values of ω. Because the modulation amplitude is an externally controlled variable, it is possible to prevent finite amplitude instabilities by limiting its growth.

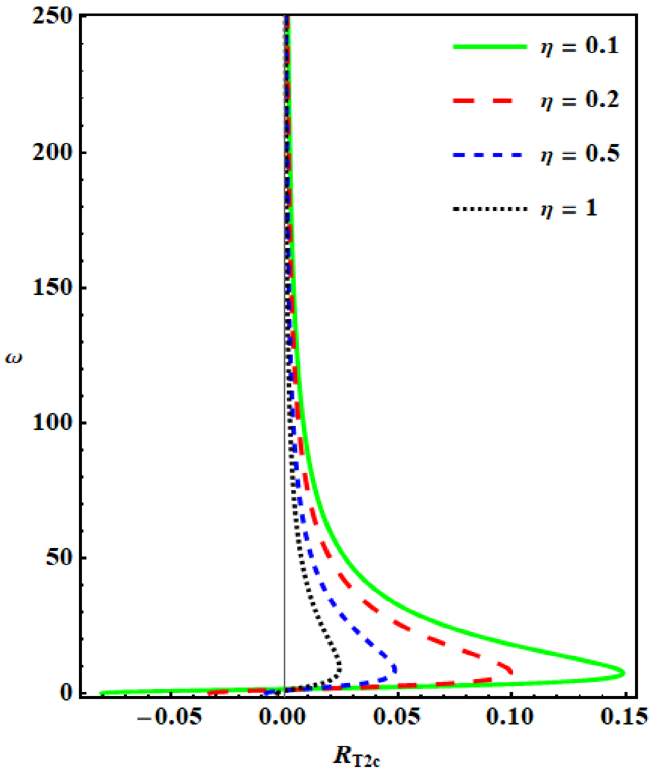

Fig. 2: Plot of $R_{T_{2c}}$ *vs* ω for different values of η with $P_{rD} = 2$, $R_{et} = 5$ and $\varepsilon = 0.5$.

Figure 1 demonstrates the effect of the Darcy-electrical Rayleigh number R_{et} on the correction Rayleigh number $R_{T_{2c}}$ with fixed values of Darcy-Prandtl number and anisotropic parameters. It is clear from this figure that, for low frequency of the modulating electric field, increasing the value of R_{et} decreases the magnitude of $R_{T_{2c}}$, and for moderate and higher frequencies, increasing the value of R_{et} increases the magnitude of $R_{T_{2c}}$. Indeed, the value of $R_{T_{2c}}$ increases negatively with the Darcy-electrical Rayleigh number R_{et} at low frequencies, but positively with the Darcy-electrical Rayleigh number at moderate and high frequencies, indicating that the effect of R_{et} is to destabilize the system at low frequencies while stabilizing the system at moderate and high values of ω. Figure 2 shows the variation of $R_{T_{2c}}$ with ω for various values of the thermal anisotropy parameter η with the Darcy-electrical Rayleigh number, Darcy-Prandtl number and mechanical anisotropy parameter fixed. If ω is small, $R_{T_{2c}}$ increases as η increases. The trend, however, reverses for moderate and large values of the frequency of electric field modulation ω. It follows that the parameter η, characterizing the thermal anisotropy of the dielectric fluid layer, is responsible for advancing the onset of electroconvection for moderate and large values of the frequency of electric field modulation and the opposite performance is observed for small values of ω.

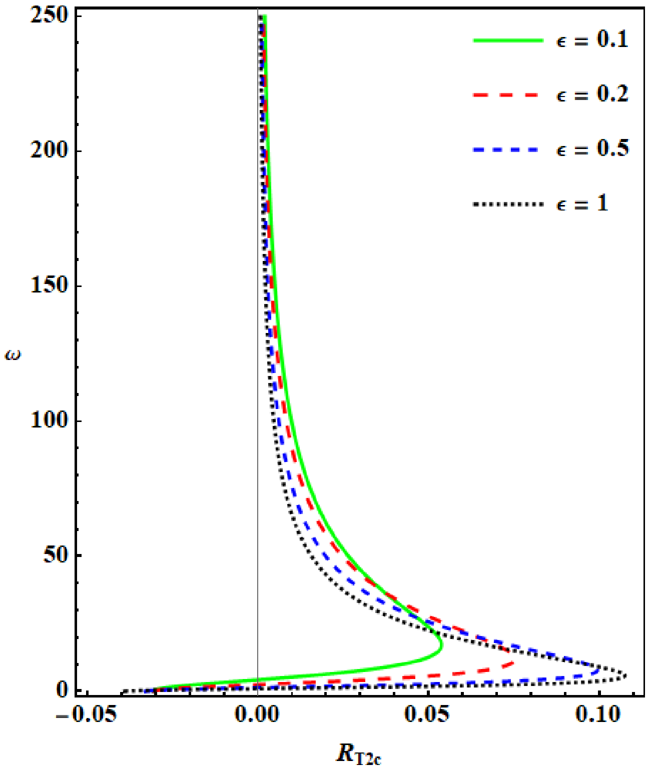

Fig. 3: Plot of $R_{T_{2c}}$ *vs* ω for different values of ε with $P_{rD} = 2$, $R_{et} = 5$ and $\eta = 0.2$.

When all other parameters are statistically controlled, Figure 3 reflects the extent of the mechanical anisotropy parameter ε on the critical correction Rayleigh number $R_{T_{2c}}$. We can see from this figure that $R_{T_{2c}}$ increases as frequency ω increases from small values indicating that mechanical anisotropy parameter ε has a stabilizing effect on convection in an electric field modulated dielectric fluid anisotropic porous medium. However, the opposite trend is seen for moderate and large values of the frequency of electric field modulation ω. Figure 4 depicts the effect of the Darcy-Prandtl number P_{rD} on the critical correction Rayleigh number $R_{T_{2c}}$ when all other parameters are fixed. This figure shows that, regardless of the range of the frequency of electric field modulation ω, an increase in the Darcy-Prandtl number P_{rD} increases the values of $R_{T_{2c}}$, indicating that the Darcy-Prandtl number on the electric field modulated fluid layer of an anisotropic porous medium is stabilizing over the entire domain of the frequency of electric field modulation except for the disappearing effect of P_{rD} when the frequency of electric field modulation ω is sufficiently large.

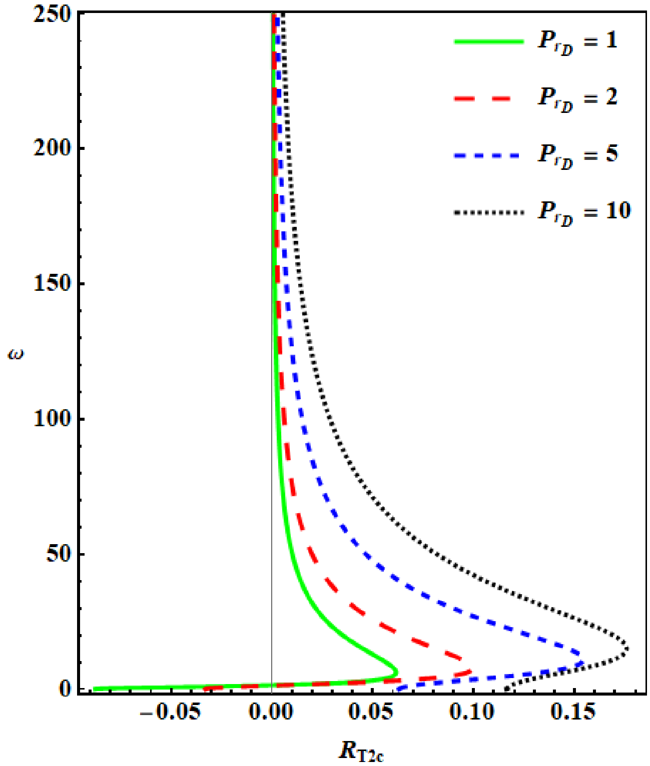

Fig. 4: Plot of $R_{T_{2c}}$ *vs* ω for different values of P_{rD} with $\varepsilon = 0.5$, $R_{et} = 5$ and $\eta = 0.2$.

7. Conclusions

The thermal convective instability of a dielectric fluid saturated densely packed anisotropic porous layer driven by the dielectrophoretic force and electric field modulation is investigated. The correction Darcy-Rayleigh number is shown to depend sensitively on the Darcy-electrical Rayleigh number, Darcy-Prandtl number, mechanical and thermal anisotropy parameters. The following conclusions are drawn from the present study:

- Subcritical convective motion is possible for low frequency modulation of the electric field and only supercritical motion exists for moderate and high frequencies of the electric field modulation in all the cases.
- The classical destabilizing effect of the dielectrophoretic force associated with the unmodulated dielectric fluid layer is only realized for low frequency modulation of the electric field.
- The dielectrophoretic force is shown to stabilize the system when the frequency of electric field modulation is moderate and large.
- The thermal and mechanical anisotropic characteristics are responsible for the enhancement of the onset of electroconvection when the frequency of electric field modulation is moderate and large.
- Delayed electrothermoconvective instability due to the presence of thermal and mechanical anisotropic characteristics is shown to be a possibility when the frequency of electric field modulation is small.
- Deferment of the threshold of electroconvection is substantiated due to the presence of densely packed porous layer through the Darcy-Prandtl number for low and moderate values of the frequency of electric field modulation.
- In all cases, the modulation effect disappears at high frequencies of the time-varying electric field.

In summary, electric field modulation in a horizontal layer of dielectric fluid saturated densely packed porous medium with anisotropic characteristics can induce or delay convection depending on the magnitude of the frequency of electric field modulation. As a result, electric field modulation mechanism can be employed to control convective instability in densely packed anisotropic porous media saturated with dielectric fluids.

8. References

[1] D. C. Jolly, J. R. Melcher, Electroconvective instability in a fluid layer, *Proceedings of the Royal Society of London. A. Mathematical and Physical Sciences,* Vol. 314, No. 1517, pp. 269-283, 1970.

[2] M. Takashima, The effect of rotation on electrohydrodynamic instability, *Canadian Journal of Physics,* Vol. 54, No. 3, pp. 342-347, 1976.

[3] R. BRADLEY, Overstable electroconvective instabilities, *The Quarterly Journal of Mechanics and Applied Mathematics,* Vol. 31, No. 3, pp. 381-390, 1978.

[4] M. Takashima, A. K. Ghosh, Electrohydrodynamic instability in a viscoelastic liquid layer, *Journal of the Physical Society of Japan,* Vol. 47, No. 5, pp. 1717-1722, 1979.

[5] A. Castellanos, P. Atten, M. Velarde, Oscillatory and steady convection in dielectric liquid layers subjected to unipolar injection and temperature gradient, *The Physics of fluids,* Vol. 27, No. 7, pp. 1607-1615, 1984.

[6] M. Takashima, The stability of natural convection in a vertical layer of electrically conducting fluid in the presence of a transverse magnetic field, *Fluid dynamics research,* Vol. 14, No. 3, pp. 121, 1994.

[7] J.-S. Chang, A. Watson, Electromagnetic hydrodynamics, *IEEE Transactions on Dielectrics and Electrical Insulation,* Vol. 1, No. 5, pp. 871-895, 1994.

[8] J. Wu, P. Traore, C. Louste, L. Dascalescu, F.-B. Tian, A. T. Perez, Effect of the mobility parameter on the oscillatory electroconvection of dielectric liquids subject to strong unipolar charge injection, *IEEE Transactions on Industry Applications,* Vol. 50, No. 4, pp. 2306-2313, 2014.

[9] S. Maruthamanikandan, S. Smita, Convective heat transfer in Maxwell-Cattaneo dielectric fluids, *Int. J. Comp. Engg. Res.,* Vol. 3, pp. 347-355, 2013.

[10] S. S. Nagouda, S. Maruthamanikandan, Rayleigh-bénard convection in a horizontal layer of porous medium saturated with a thermally radiating dielectric fluid, *International Journal of Computational Engineering Research,* Vol. 11, No. 3, pp. 1-10, 2015.

[11] Z. Lu, G. Liu, B. Wang, Flow structure and heat transfer of electro-thermo-convection in a dielectric liquid layer, *Physics of Fluids,* Vol. 31, No. 6, pp. 064103, 2019.

[12] M. Mohammadi, A. Farajpour, A. Moradi, M. Hosseini, Vibration analysis of the rotating multilayer piezoelectric Timoshenko nanobeam, *Engineering Analysis with Boundary Elements,* Vol. 145, pp. 117-131, 2022.

[13] M. Mohammadi, A. Rastgoo, Primary and secondary resonance analysis of FG/lipid nanoplate with considering porosity distribution based on a nonlinear elastic medium, *Mechanics of Advanced Materials and Structures,* Vol. 27, No. 20, pp. 1709-1730, 2020.

[14] M. Mohammadi, M. Hosseini, M. Shishesaz, A. Hadi, A. Rastgoo, Primary and secondary resonance analysis of porous functionally graded nanobeam resting on a nonlinear foundation subjected to mechanical and electrical loads, *European Journal of Mechanics-A/Solids,* Vol. 77, pp. 103793, 2019.

[15] M. Mohammadi, A. Rastgoo, Nonlinear vibration analysis of the viscoelastic composite nanoplate with three directionally imperfect porous FG core, *Structural Engineering and Mechanics, An Int'l Journal,* Vol. 69, No. 2, pp. 131-143, 2019.

[16] A. Farajpour, A. Rastgoo, M. Mohammadi, Vibration, buckling and smart control of microtubules using piezoelectric nanoshells under electric voltage in thermal environment, *Physica B: Condensed Matter,* Vol. 509, pp. 100-114, 2017.

[17] A. Farajpour, M. H. Yazdi, A. Rastgoo, M. Loghmani, M. Mohammadi, Nonlocal nonlinear plate model for large amplitude vibration of magneto-electro-elastic nanoplates, *Composite Structures,* Vol. 140, pp. 323-336, 2016.

[18] A. Farajpour, M. Yazdi, A. Rastgoo, M. Mohammadi, A higher-order nonlocal strain gradient plate model for buckling of orthotropic nanoplates in thermal environment, *Acta Mechanica,* Vol. 227, No. 7, pp. 1849-1867, 2016.

[19] M. Mohammadi, M. Safarabadi, A. Rastgoo, A. Farajpour, Hygro-mechanical vibration analysis of a rotating viscoelastic nanobeam embedded in a visco-Pasternak elastic medium and in a nonlinear thermal environment, *Acta Mechanica,* Vol. 227, No. 8, pp. 2207-2232, 2016.

[20] M. R. Farajpour, A. Rastgoo, A. Farajpour, M. Mohammadi, Vibration of piezoelectric nanofilm-based electromechanical sensors via higher-order non-local strain gradient theory, *Micro & Nano Letters,* Vol. 11, No. 6, pp. 302-307, 2016.

[21] M. Baghani, M. Mohammadi, A. Farajpour, Dynamic and stability analysis of the rotating nanobeam in a nonuniform magnetic field considering the surface energy, *International Journal of Applied Mechanics,* Vol. 8, No. 04, pp. 1650048, 2016.

[22] M. Goodarzi, M. Mohammadi, M. Khooran, F. Saadi, Thermo-mechanical vibration analysis of FG circular and annular nanoplate based on the visco-pasternak foundation, *Journal of Solid Mechanics,* Vol. 8, No. 4, pp. 788-805, 2016.

[23] H. Asemi, S. Asemi, A. Farajpour, M. Mohammadi, Nanoscale mass detection based on vibrating piezoelectric ultrathin films under thermo-electro-mechanical loads, *Physica E: Low-dimensional Systems and Nanostructures,* Vol. 68, pp. 112-122, 2015.

[24] M. Safarabadi, M. Mohammadi, A. Farajpour, M. Goodarzi, Effect of surface energy on the vibration analysis of rotating nanobeam, 2015.

[25] M. Goodarzi, M. Mohammadi, A. Gharib, Techno-Economic Analysis of Solar Energy for Cathodic Protection of Oil and Gas Buried Pipelines in Southwestern of Iran, in *Proceeding of,* https://publications.waset.org/abstracts/33008/techno-economic-analysis-of …, pp.

[26] M. Mohammadi, A. A. Nekounam, M. Amiri, The vibration analysis of the composite natural gas pipelines in the nonlinear thermal and humidity environment, in *Proceeding of,* https://civilica.com/doc/540946/, pp.

[27] M. Goodarzi, M. Mohammadi, M. Rezaee, Technical Feasibility Analysis of PV Water Pumping System in Khuzestan Province-Iran, in *Proceeding of,* https://publications.waset.org/abstracts/18930/technical-feasibility …, pp.

[28] M. Mohammadi, A. Farajpour, A. Moradi, M. Ghayour, Shear buckling of orthotropic rectangular graphene sheet embedded in an elastic medium in thermal environment, *Composites Part B: Engineering,* Vol. 56, pp. 629-637, 2014.

[29] M. Mohammadi, A. Moradi, M. Ghayour, A. Farajpour, Exact solution for thermo-mechanical vibration of orthotropic mono-layer graphene sheet embedded in an elastic medium, *Latin American Journal of Solids and Structures,* Vol. 11, pp. 437-458, 2014.

[30] M. Mohammadi, A. Farajpour, M. Goodarzi, F. Dinari, Thermo-mechanical vibration analysis of annular and circular graphene sheet embedded in an elastic medium, *Latin American Journal of Solids and Structures,* Vol. 11, pp. 659-682, 2014.

[31] M. Mohammadi, A. Farajpour, M. Goodarzi, Numerical study of the effect of shear in-plane load on the vibration analysis of graphene sheet embedded in an elastic medium, *Computational Materials Science,* Vol. 82, pp. 510-520, 2014.

[32] A. Farajpour, A. Rastgoo, M. Mohammadi, Surface effects on the mechanical characteristics of microtubule networks in living cells, *Mechanics Research Communications,* Vol. 57, pp. 18-26, 2014.

[33] S. R. Asemi, M. Mohammadi, A. Farajpour, A study on the nonlinear stability of orthotropic single-layered graphene sheet based on nonlocal elasticity theory, *Latin American Journal of Solids and Structures,* Vol. 11, pp. 1541-1546, 2014.

[34] M. Goodarzi, M. Mohammadi, A. Farajpour, M. Khooran, Investigation of the effect of pre-stressed on vibration frequency of rectangular nanoplate based on a visco-Pasternak foundation, 2014.

[35] S. Asemi, A. Farajpour, H. Asemi, M. Mohammadi, Influence of initial stress on the vibration of double-piezoelectric-nanoplate systems with various boundary conditions using DQM, *Physica E: Low-dimensional Systems and Nanostructures,* Vol. 63, pp. 169-179, 2014.

[36] S. Asemi, A. Farajpour, M. Mohammadi, Nonlinear vibration analysis of piezoelectric nanoelectromechanical resonators based on nonlocal elasticity theory, *Composite Structures,* Vol. 116, pp. 703-712, 2014.

[37] M. Mohammadi, M. Ghayour, A. Farajpour, Free transverse vibration analysis of circular and annular graphene sheets with various boundary conditions using the nonlocal continuum plate model, *Composites Part B: Engineering,* Vol. 45, No. 1, pp. 32-42, 2013.

[38] M. Mohammadi, M. Goodarzi, M. Ghayour, A. Farajpour, Influence of in-plane pre-load on the vibration frequency of circular graphene sheet via nonlocal continuum theory, *Composites Part B: Engineering,* Vol. 51, pp. 121-129, 2013.

[39] M. Mohammadi, A. Farajpour, M. Goodarzi, R. Heydarshenas, Levy type solution for nonlocal thermo-mechanical vibration of orthotropic mono-layer graphene sheet embedded in an elastic medium, *Journal of Solid Mechanics,* Vol. 5, No. 2, pp. 116-132, 2013.

[40] M. Mohammadi, A. Farajpour, M. Goodarzi, H. Mohammadi, Temperature Effect on Vibration Analysis of Annular Graphene Sheet Embedded on Visco-Pasternak Foundati, *Journal of Solid Mechanics,* Vol. 5, No. 3, pp. 305-323, 2013.

[41] M. Danesh, A. Farajpour, M. Mohammadi, Axial vibration analysis of a tapered nanorod based on nonlocal elasticity theory and differential quadrature method, *Mechanics Research Communications,* Vol. 39, No. 1, pp. 23-27, 2012.

[42] A. Farajpour, A. Shahidi, M. Mohammadi, M. Mahzoon, Buckling of orthotropic micro/nanoscale plates under linearly varying in-plane load via nonlocal continuum mechanics, *Composite Structures*, Vol. 94, No. 5, pp. 1605-1615, 2012.

[43] M. Mohammadi, M. Goodarzi, M. Ghayour, S. Alivand, Small scale effect on the vibration of orthotropic plates embedded in an elastic medium and under biaxial in-plane pre-load via nonlocal elasticity theory, 2012.

[44] A. Farajpour, M. Mohammadi, A. Shahidi, M. Mahzoon, Axisymmetric buckling of the circular graphene sheets with the nonlocal continuum plate model, *Physica E: Low-dimensional Systems and Nanostructures*, Vol. 43, No. 10, pp. 1820-1825, 2011.

[45] A. Farajpour, M. Danesh, M. Mohammadi, Buckling analysis of variable thickness nanoplates using nonlocal continuum mechanics, *Physica E: Low-dimensional Systems and Nanostructures*, Vol. 44, No. 3, pp. 719-727, 2011.

[46] H. Moosavi, M. Mohammadi, A. Farajpour, S. Shahidi, Vibration analysis of nanorings using nonlocal continuum mechanics and shear deformable ring theory, *Physica E: Low-dimensional Systems and Nanostructures*, Vol. 44, No. 1, pp. 135-140, 2011.

[47] M. Mohammadi, M. Ghayour, A. Farajpour, Analysis of free vibration sector plate based on elastic medium by using new version differential quadrature method, *Journal of solid mechanics in engineering*, Vol. 3, No. 2, pp. 47-56, 2011.

[48] A. Farajpour, M. Mohammadi, M. Ghayour, Shear buckling of rectangular nanoplates embedded in elastic medium based on nonlocal elasticity theory, in *Proceeding of*, www.civilica.com/Paper-ISME19-ISME19_390.html, pp. 390.

[49] M. Mohammadi, A. Farajpour, A. R. Shahidi, Higher order shear deformation theory for the buckling of orthotropic rectangular nanoplates using nonlocal elasticity, in *Proceeding of*, www.civilica.com/Paper-ISME19-ISME19_391.html, pp. 391.

[50] M. Mohammadi, A. Farajpour, A. R. Shahidi, Effects of boundary conditions on the buckling of single-layered graphene sheets based on nonlocal elasticity, in *Proceeding of*, www.civilica.com/Paper-ISME19-ISME19_382.html, pp. 382.

[51] M. Mohammadi, M. Ghayour, A. Farajpour, Using of new version integral differential method to analysis of free vibration orthotropic sector plate based on elastic medium, in *Proceeding of*, www.civilica.com/Paper-ISME19-ISME19_497.html, pp. 497.

[52] N. Ghayour, A. Sedaghat, M. Mohammadi, Wave propagation approach to fluid filled submerged visco-elastic finite cylindrical shells, 2011.

[53] M. Mohammadi, A. Farajpour, A. Rastgoo, Coriolis effects on the thermo-mechanical vibration analysis of the rotating multilayer piezoelectric nanobeam, *Acta Mechanica*, https://doi.org/10.1007/s00707-022-03430-0, 2023.

[54] R. Wooding, *Large-scale geothermal field parameters and convection theory*, Applied Mathematics Division, DSIR, Wellington, New Zealand, pp. 1976.

[55] J. Epherre, CRITERE D'APPARITION DE LA CONVECTION NATURELLE DANS UNE COUCHE POREUSE ANISOTROPE, 1975.

[56] S. M. Alex, P. R. Patil, Effect of a variable gravity field on convection in an anisotropic porous medium with internal heat source and inclined temperature gradient, *J. Heat Transfer*, Vol. 124, No. 1, pp. 144-150, 2002.

[57] M. Malashetty, D. Basavaraja, Rayleigh–Benard convection subject to time dependent wall temperature/gravity in a fluid-saturated anisotropic porous medium, *Heat and mass transfer*, Vol. 38, No. 7, pp. 551-563, 2002.

[58] M. Malashetty, B. S. Biradar, The onset of double diffusive reaction-convection in an anisotropic porous layer, *Physics of Fluids*, Vol. 23, No. 6, pp. 064102, 2011.

[59] N. M. Thomas, S. Maruthamanikandan, Effect of gravity modulation on the onset of ferroconvection in a densely packed porous layer, *IOSR J Appl Phys*, Vol. 3, pp. 30-40, 2013.

[60] N. A. M. Shamsudin, N. F. M. Mokhtar, Onset of Convection in a Dielectric Nanofluid Saturated Anisotropic Porous Medium.

[61] M. Takashima, H. Hamabata, The stability of natural convection in a vertical layer of dielectric fluid in the presence of a horizontal ac electric field, *Journal of the Physical Society of Japan*, Vol. 53, No. 5, pp. 1728-1736, 1984.

[62] V. Semenov, Parametric instability of a nonuniformly heated horizontal layer of liquid dielectric in a variable electric field, *Fluid dynamics*, Vol. 28, No. 5, pp. 734-735, 1993.

[63] M. Velarde, B. Smorodin, Convective instability of a plane horizontal layer of weakly conducting fluid in alternating and modulated electric fields, *Fluid dynamics,* Vol. 35, No. 3, pp. 339-345, 2000.

[64] C. Rudresha, C. Balaji, V. V. Shree, S. Maruthamanikandan, Effect of Electric Field Modulation on Electroconvection in a Dielectric Fluid-Saturated Porous Medium, *Journal of Mines, Metals and Fuels,* pp. 35-41, 2022.

[65] C. Rudresha, C. Balaji, V. V. Shree, S. Maruthamanikandan, Effect of Electric Field Modulation on The Onset of Electroconvection in a Couple Stress Fluid, *East European Journal of Physics*, No. 4, pp. 104-111, 2022.